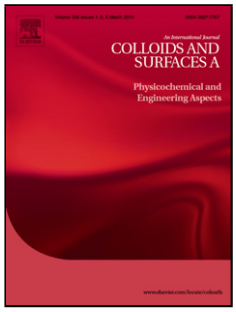


# Stability and characterization studies of Span 80 niosomes modified with CTAB in the presence of NaCl

Lara Roque (Validation) (Investigation) (Formal analysis), María Fernández (Investigation) (Resources), José M. Benito (Conceptualization) (Formal analysis) (Supervision), Isabel Escudero (Conceptualization) (Project administration) (Funding acquisition) (Writing - original draft) (Writing - review and editing)

PII: S0927-7757(20)30592-6

DOI: https://doi.org/10.1016/j.colsurfa.2020.124999

Reference: COLSUA 124999

To appear in: *Colloids and Surfaces A: Physicochemical and Engineering Aspects*

Received Date: 25 March 2020

Revised Date: 10 May 2020

Accepted Date: 11 May 2020

Please cite this article as: Roque L, Fernández M, Benito JM, Escudero I, Stability and characterization studies of Span 80 niosomes modified with CTAB in the presence of NaCl, *Colloids and Surfaces A: Physicochemical and Engineering Aspects* (2020), doi: https://doi.org/10.1016/j.colsurfa.2020.124999

# Stability and characterization studies of Span 80 niosomes modified with CTAB in the presence of NaCl

**Lara Roque, María Fernández, José M. Benito, Isabel Escudero***

Department of Biotechnology and Food Science, University of Burgos, Plaza Misael Bañuelos s/n, 09001 Burgos, Spain

E-mail addresses: lrv0010@universidaddeburgos.es (L. Roque), mfl0024@alu.ubu.es (M. Fernández), jmbmoreno@ubu.es (J.M. Benito)

*Corresponding author. Tel.: +34 947258809; fax: +34 947258831. E-mail address: iescuder@ubu.es

**Graphical Abstract**

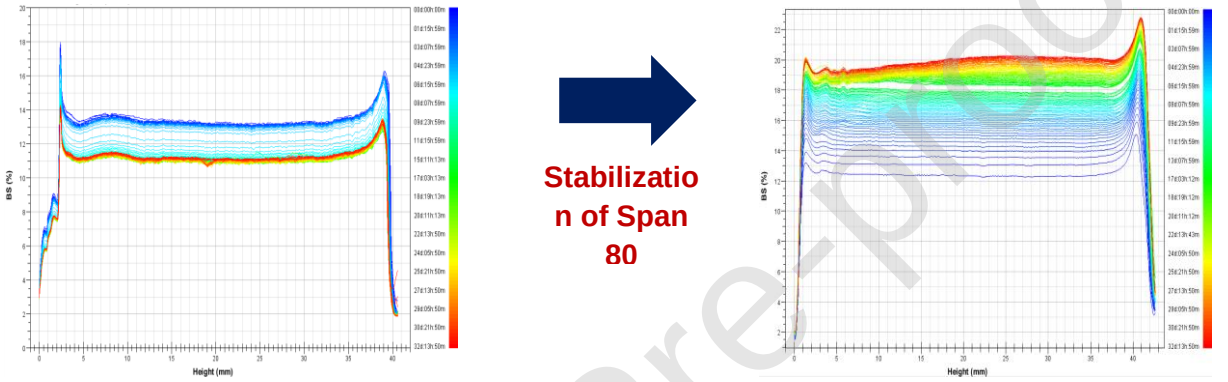


**Abstract**

This work reports the study of surface and aggregation properties of formulations containing mixed niosomes of the non-ionic surfactant sorbitan monooleate (Span 80) and the cationic surfactant cetyltrimethylammonium bromide (CTAB), in concentrations of 20 and 4 mol/m$^3$, respectively, in salt-free water and in the presence of NaCl (20, 50 and 80 mol/m$^3$). The aim of this work was the formulation of stable Span 80 and CTAB mixed niosomes with low surfactant concentration. The mixed niosomes were prepared by ultrasonication and their properties (surface tension, particle size distribution, ζ-potential, stability over time and morphology) were measured using different techniques. Data were analyzed and compared with those of the individual surfactants. Experimental results show that the addition of salt decreased the critical micelle concentration (CMC) and the surface tension of the surfactant dispersions with relation to their free-salt formulations. The presence of CTAB in the mixed niosome bilayer decreased the particle size and increased the stability of the mixed niosomes in all the formulations studied, compared with those of single Span 80. Synergism between both surfactants was obtained in the formation of niosome bilayers for formulations in pure water and with 20 and 50 mol/m$^3$ of salt, while antagonism was observed in that of 80 mol/m$^3$ NaCl. These results may allow the use of CTAB adsorbed on mixed niosomes in industrial applications, taking advantage of its antiseptic and antibacterial properties and solving the limitation imposed by its high Krafft temperature.

**Keywords**: Niosomes; Span 80; CTAB; Surfactants; Stability; Synergism.

## 1. Introduction

Niosomes are vesicles formed by self-assembly of non-ionic surfactants in aqueous media that results in closed bilayer structures. Their use has increased considerably in recent years due to their practical applications in many fields, such as medicine, cosmetics, food and pharmaceuticals, mainly due to their ability to microencapsulate compounds of different nature. They can be an alternative to liposomes due to their biological compatibility, high purity, greater chemical stability, low toxicity, low cost and better handling and storage [1–4]. Also, the use of niosomes as extraction agents of solutes present at very low concentration in aqueous solutions is a new application in the field of sustainable processes that has been explored in previous works [5–7].

The formation of stable niosomes is a non-spontaneous process that needs some energy input, so different techniques have been used to form these vesicles [8–10]. Sonication was used in this work, since it is an easy and fast technique, and does not involve the use of organic solvents.

There are a large number of non-ionic surfactants available, which are non-toxic and relatively low-cost materials for niosomes design, greatly increasing the attractiveness of these vesicles for industrial production [3,11]. In general, vesicle formation without additives occurs for surfactants with a very low hydrophilic-lipophilic balance (HLB) at a relatively high surfactant concentration [12,13]. Sorbitan monooleate (Span 80) is an attractive surfactant because it is generally recognized as safe (GRAS) by FDA, biodegradable, biocompatible and non-toxic, features that make it ideal for use in pharmaceutical, cosmetic and food industry. It has a HLB value of 4.3 and can form stable niosomes with addition of small quantities of additives as ionic surfactants [7] or cholesterol, widely used in formulations to increase the membrane rigidity [14]. However, the study on its surface and bulk behavior has hardly been investigated.

Cetyltrimethylammonium bromide (CTAB) is a cationic surfactant with effective antiseptic properties against bacteria and fungi, which is used in pharmaceutical, cosmetic and food industries [15]. Micelles are formed above a certain surfactant concentration named critical micelle concentration (CMC). Above the CMC, the surfactants form micelles which favors their practical use as encapsulation agents [16,17], drug deliver [18,19] or toxic waste removal systems [20].

The adding of additives into associate structure of surfactants will change their physicochemical characteristics, for instance, the degree of ionization, reaction rates, clouding or phase separation [21–23]. It is well known that CMC of surfactants depends on the electrolyte presence and temperature because they affect micellization and surface properties. Electrolytes affect the adsorption of surfactant monomers at the air-water interface because of the decrease of electrostatic repulsions and consequently the surface tension [19]. Many works [24–26] show the CMC decreasing of CTAB with salt addition, particularly Roy et al. [25] proved that CMC decreases from 0.98 mol/m$^3$ in pure water to 0.47 mol/m$^3$ in 10 mol/m$^3$ NaCl solution, both at 25 °C.

Moreover, ionic surfactants work effectively only above a critical temperature called Krafft temperature ($T_k$). The $T_K$ is generally conceived as the melting temperature of a hydrated solid surfactant [3]. Addition of inorganic electrolytes usually lowers the CMC of surfactants and the surface activity; however, its effect on $T_k$ is not clear and depends on the ion common presence. Roy et al. [25] showed that the $T_k$ of CTAB gradually decreases and increases from 24.8 °C in pure water with increasing the concentration of $Cl^-$ and $Br^-$, respectively. This fact shows that the addition of NaCl in CTAB formulations definitely favors their practical use.

The decrease of CMC and $T_k$ and the simultaneous increase of stability of formulations is the subject of active research, since both industries and consumers demand to minimize the amount of surfactant used in the different formulations for health, economic and environmental reasons [27]. In addition to electrolytes [28–30], the use of other additives such as alcohols, sugars, or mixed surfactant systems are also widely investigated due to their possible synergistic behavior that improves their properties and promotes new applications [31–33].

The present work focuses on the mixed niosomes of the cationic surfactant CTAB and the non-ionic surfactant Span 80. Mixed niosomes were formed by sonication of 20 mol/m$^3$ Span 80 and 4 mol/m$^3$ CTAB formulations, which are below the saturation line in the pseudo-phase equilibrium diagram of solubilization of Span 80 niosomes by CTAB. The mixtures in pure water and NaCl solutions were analyzed by several techniques to evaluate their aggregation and surface properties compared to those of the single surfactants. This work may be of considerable interest from practical and fundamental points of view regarding the formulations of these mixed systems for their possible use in multiple applications.

## 2. Materials and methods

### *2.1. Chemicals*

The non-ionic surfactant sorbitan monooleate ($C_{24}H_{44}O_6$, Span 80, Sigma-Aldrich), the cationic surfactant cetyltrimethylammonium bromide ($C_{19}H_{42}NBr$, CTAB, 98%, Sigma-Aldrich) and sodium hydroxide (analysis grade, Scharlau) were used as supplied. Ultrapure deionized Milli-Q water (Millipore, USA), with a conductivity of 0.1 μS/cm, was used for the preparation of all solutions.

### *2.2. Solubilization experiments of Span 80 niosomes by CTAB*

Aqueous solutions of single surfactants (Span 80 and CTAB) were prepared 24 h before use, in order to hydrate and relax the carbonated chains of their molecular structures, weighing the exact amounts of each surfactant on an analytical balance (Sartorius, accurate to ± 0.0001 g), and water addition up to a final volume of 100 cm$^3$.

Span 80 niosomes were prepared by direct ultrasonication of 10 cm$^3$ aqueous solutions of Span 80 (5, 10, 15 and 20 mol/m$^3$). The application of ultrasounds was carried out over a 10 min effective time, with pulses every 5 s (5 s on and 5 s off, 60 cycles; 30% amplitude, 500 W), to avoid overheating of the sample, using a high-intensity ultrasonic processor (Vibra-Cell VCX 500, Sonics & Materials Inc., USA) equipped with a 3 mm-diameter titanium alloy bicylindrical probe. Subsequently, the samples were centrifuged (Eppendorf 5804 centrifuge) in 15 cm$^3$ polystyrene centrifuge tubes for 45 min at 9000 rpm, in order to remove traces of metal detached from the probe.

Niosome solubilization experiments were carried out in 20 cm$^3$ blisters by contacting 10 cm$^3$ of each niosome suspension (5, 10, 15 and 20 mol/m$^3$ of Span 80 in water) with different volumes of 25 or 50 mol/m$^3$ CTAB aqueous solutions. CTAB concentration in samples was between 0–24 mol/m$^3$. Samples were maintained in an incubator shaker (Model G25, New Brunswick Scientific Co.) at 150 rpm and 25 °C during predetermined periods of time (24–72 h), after which they were analyzed by the under mentioned techniques.

### *2.3. Mixed niosomes formulation*

Mixed niosomes of Span 80 (20 mol/m$^3$) and CTAB (4 mol/m$^3$) were formulated by mixing appropriate volumes of the single surfactant solutions, previously prepared in water or in sodium chloride aqueous solutions (20, 50 and 80 mol/m$^3$ of NaCl), applying ultrasounds for 10 min and centrifugation, as described above. This formulation was chosen in light of the solubilization results of niosomes with CTAB, as will be explained below. Furthermore, for comparative purposes, the formulations of the individual surfactants (Span 80 niosomes or CTAB micelles suspensions) were also analyzed without salt and in the presence of the same salt concentrations as mentioned above.

### *2.4. Analytical techniques*

*Optical density*. A total sample volume of 1.2 $cm^3$ was placed in a quartz cuvette (10 × 10 mm) and its optical density (OD) was measured at a 350 nm wavelength using a double beam UV-vis spectrophotometer (Hitachi U-2000). Milli-Q water was used as blank. Previously, it was checked that the optical density at 350 nm wavelength provided a good sensitivity to the turbidity caused by the presence of niosomes, whose size is much larger than that of the micelles. The same wavelength was used in previous work on Span 80 niosomes solubilization by SDS [34].

*Particle size distribution*. The mean hydrodynamic diameter (Z-average) and the polydispersity index (PDI) of the samples were measured by dynamic light scattering (DLS) using a Zetasizer Nano ZS apparatus (Malvern Instruments Ltd., UK).

*ζ-Potential*. Measurements were conducted with the aforementioned Zetasizer Nano ZS apparatus, using the Laser Doppler Velocimetry technique. They were performed on the same sample previously prepared to measure the particle size, but using the appropriate cell equipped with electrodes to allow the passage of electric current.

*Morphological analysis*. It was performed by negative staining transmission electron microscopy (NS-TEM), using a JEOL-2000 EX-II TEM operating at 160–180 kV, with an image resolution of 1 nm.

The detailed description of the above mentioned techniques can be found in a previous work [34].

*Surface tension*. It was measured using an optical tensiometer (Attension Theta 200 Basic Model, Biolin Scientific Ltd.) by the drop shape analysis method at 20 °C. The apparatus is controlled by a computer equipped with pendant drop shape image analysis software. Each sample was analyzed over time. The time needed to reach equilibrium was between 5 and 30 min, depending on the surfactant concentration in the sample. The instrument was calibrated daily using a 4 mm diameter standard tungsten ball to adjust camera parameters and checking the surface tension of distilled water ($\gamma$ = 72 mN/m). Dispersions containing CTAB (10 $mol/m^3$) micelles, Span 80 (20 $mol/m^3$) niosomes, or mixed niosomes of Span 80 (20 $mol/m^3$) and CTAB (4 $mol/m^3$), in water or sodium chloride solutions were diluted with the same solvent and maintained in an incubator shaker at 150 rpm and 25 °C for 24 h. Surface tension measurements were repeated at least twice to check the reproducibility. Surface tension data *vs.* time were used for the dynamic analysis of the surface tension in order to verify the existence of barrier effects to the surfactant adsorption at the interface. Equilibrium surface tension data *vs* logarithm of surfactant concentration were used to determine the CMC of each formulation.

*Stability measurement.* Formulation stability was determined with a Turbiscan Lab Expert (Formulaction Co., France) by static multiple light scattering (S-MLS). The samples (20 mL) were placed without dilution in cylindrical glass cells where a near infrared light of 880 nm wavelength passes through them upward at pre-set time intervals. Backscattered (BS) light was monitored as a function of sample height in the cell (about 40 mm) at 25 °C every 5 h for 7 days, and later every 24 h for 34 days. BS value depends on the wavelength of the incident light. BS intensity increases with the concentration and the particle size for particles smaller than the incident wavelength. However, when the particles are larger than the incident wavelength (> 0.8 μm), the BS will decrease as the particle size increases [35–37].

## 3. Results and discussion

### *3.1. Solubilization of Span 80 niosomes by CTAB*

Fig. 1 shows optical density (OD) at 350 nm wavelength of samples containing 20 $mol/m^3$ Span 80 niosomes after prefixed contact times (24, 48 and 72 h) with different amount of CTAB (0–24 $mol/m^3$).

Solubilization curves by CTAB of 5, 10 and 15 mol/m$^3$ Span 80 niosomes are available in Fig. S1 (supplementary data). It is observed in all Span 80 formulations (Figs. 1 and S1) that the OD curves measured at different contact time (24–72 h) are coincident, indicating fast solubilization processes. In the niosome solubilization curves, the point of maximum OD corresponds to the saturation of the niosomes with CTAB; however, the minimum OD corresponds to the complete solubilization, where there is no presence of niosomes. Between the two points both niosomes and mixed micelles, together with surfactant monomers, coexist in the equilibrium dispersions. Critical saturation and complete solubilization points of niosomes move towards higher CTAB concentrations as the concentration of Span 80 increases. The composition of the saturation critical points is confirmed by analysis of the particle size distribution shown in Figs. 2 and S2. In these figures, it is possible to discern a first zone at the lower CTAB concentrations, where values of PDI $\leq$ 0.3 indicate fairly homogeneous population in particle size, followed by a second zone with PDI $\geq$ 0.4 indicating heterogeneous population in particle size due to mixed micelles formation. The boundary line between both zones corresponds to 0, 2, 4, and 6 mol/m$^3$ of CTAB for the 5, 10, 15, and 20 mol/m$^3$ Span 80 formulations, respectively, which are consistent with the saturation points observed from OD data.

The points of saturation and total micellization are depicted in the pseudo-phase equilibrium diagram shown in Fig. 3. The union of the critical points of saturation and solubilization follows straight lines, according to the behavior observed in the bibliography [34,38,39]. These lines separate zones with different structures: mixed niosomes in zone below the saturation line, coexistence of niosomes and micelles in zone between both lines, and mixed micelles above the solubilization line. Some authors [40,41] have verified the formation of mixed micelles during the adsorption stage.

### *3.2. Effect of NaCl on aggregation and surface properties*

In view of the pseudo-phase diagram shown in Fig. 3, the formulation of Span 80 (20 mol/m$^3$) and CTAB (4 mol/m$^3$), just below the saturation line, was selected for stable mixed niosomes formation and to determine their aggregation and surface properties. The presence of different NaCl concentrations in the formulations was also studied due to its great interest in several food and biotechnological applications.

Figs. 4, 5, and 6 depict the surface tension curves of individual and mixed surfactants (in a 4/20 molar ratio of CTAB/Span 80), respectively. The surface tension curves were used to calculate the points of inflection which correspond to the critical micelle concentration (CMC) and the surface tension at the CMC ($\gamma_{CMC}$).

Additional parameters were studied to evaluate the effect of NaCl on formulations. The surface tension reduction effectiveness ($\pi_{CMC}$), the adsorption efficiency ($pC_{20}$), the maximum surface excess concentration in the air-water interface ($\Gamma_{max}$), the minimum area per molecule in the adsorption layer ($A_{min}$), the standard Gibbs free energy change of micellization ($\Delta G^0_m$), and the standard Gibbs free energy change of adsorption ($\Delta G^0_{ads}$) were calculated using the following equations [41–43]:

$$\pi_{CMC} = \gamma_0 - \gamma_{CMC} \quad (1)$$

$$pC_{20} = (\pi_{CMC} - 20)/2.303nRT\Gamma_{max} - \log CMC \quad (2)$$

$$\Gamma_{max} = -(1/(2.303nRT))(\partial\gamma/\partial logC) \quad (3)$$

$$A_{min} = 10^{20}/N_A\Gamma_{max} \quad (4)$$

$$\Delta G^0{}_m = (2-\alpha)RTlnx_{CMC} \quad (5)$$

$$\Delta G^0{}_{ads} = \Delta G^0{}_m - (\pi_{CMC}/\Gamma_{max}) \quad (6)$$

where $\gamma_0$ is the surface tension of water (72 mN/m), R = 8.314 N m/(mol K) is the ideal gas constant, $N_A$ = 6.023 $10^{23}$ molecules/mol is the Avogadro's constant, T = 298.15 K is the temperature, $x_{CMC}$ is the mole fraction of the surfactant at the CMC ($x_{CMC}$ = CMC/55.55, with CMC expressed in molar concentration), and ∂γ/∂logC is the slope below the CMC in the surface tension plots. The parameter "n" in Eqs. 2 and 3 depends on the number of species constituting the adsorption layer, being n = 1 for non-ionic surfactants, and n = 2 for 1:1 ionic surfactants considering full ionization and absence of electrolytes; however, in presence of high concentration of electrolytes, n = 1 [44]. In this work, the following values of n were used: for CTAB in water, the degree of counterion dissociation ($\alpha$) was taken equal to 0.26 [45], and n was 2–0.26 = 1.74. For CTAB in presence of NaCl, n = 1. For the mixed system CTAB/Span 80 (4/20 molar ratio) n was estimated with those values used for the single surfactants multiplied by their mole fractions in the formulation, that is: $\alpha$ = 0.17 × 0.26 = 0.04 and n = 0.17 × 1.74 + 0.83 = 1.12 for the mixed system in pure water, and $\alpha$ = 0 and n = 1 for mixed systems with salt. Results are shown in Table 1.

The existence of barrier effects to the adsorption at the air-liquid interface was verified by analysis of the surface tension variation over time. The equilibrium times were comparatively shorter as the salt content in the formulations increased. Adsorption dynamic curves were analyzed by the Wars-Torday model based on diffusion controlled adsorption mechanism (Eq. 7), and particularly by their analytical solutions at short time (t→0) and long time (t→∞) expressed by Eqs. 8 and 9, respectively [45].

$$\Gamma_{(t)} = 2\sqrt{\frac{D}{\pi}}\left[C_0 t^{1/2} - \int_0^{\sqrt{t}} C_s d\sqrt{t-\tau}\right] \quad (7)$$

$$\gamma_{(t)\,t\to 0} = \gamma_0 - 2nRTC_0\sqrt{\frac{Ds\,t}{\pi}} \quad (8)$$

$$\gamma_{(t)\,t\to\infty} = \gamma_{eq} + \frac{nRT\,\Gamma_{max}^2}{C_0}\sqrt{\frac{\pi}{4D_{ef}t}} \quad (9)$$

where $\gamma_{(t)\,t\to0}$ and $\gamma_{(t)\,t\to\infty}$ are surface tensions at short time and long time, respectively, $D_s$ and $D_{ef}$ are the monomer diffusion and back-diffusion coefficients, $\gamma_0$ and $\gamma_{eq}$ are the equilibrium surface tension of water and the formulation, $C_0$ is the bulk surfactant concentration and $C_S$ and $\tau$ in Eq. 7 are the concentration in the subsurface and a dummy variable of integration, respectively.

Eqs. 8 and 9 represent a linear behavior of $\gamma_{(t)\,t\to0}$ and $\gamma_{(t)\,t\to\infty}$ data as a function of $t^{1/2}$ and $t^{-1/2}$, respectively. $D_s$ and $D_{ef}$ were calculated through the gradients of the fitted lines obtained from these plots by using the following equations:

$$D_s = \left[\frac{grad_1\pi^{1/2}}{2\,n\,R\,T\,C_0}\right]^2 \quad (10)$$

$$D_{ef} = \left[\frac{n\,R\,T\,\Gamma_{max}^2\,\pi^{1/2}}{2\,C_0 grad_2}\right]^2 \quad (11)$$

Results of $D_s$ and $D_{ef}$ are shown in Table 2. $D_{ef}/D_s$ ratio values close to 1 mean that adsorption of surfactant monomers at the air-liquid interface is controlled by their diffusion, without the existence of barrier effects to adsorption. However, values of $D_{ef}$ lower than $D_s$ mean that diffusion to the air-liquid interface from an imaginary subsurface very close to the interface, slows down as the interface becomes more crowded.

*3.2.1. Effect of NaCl on CTAB micelles*

Data in Table 1 for CTAB in pure water agree with those published in several works [44,46,47]. It is also observed in Table 1 that the CMC of the CTAB surfactant decreases as the salt concentration increases, indicating a decrease in the concentration of monomers in solution, which may be due to the screening between the polar heads of the CTAB monomers produced by the $Cl^-$ ions, lowering their stability in solution and promoting micellization. The screening effect that provides the presence of salt also occurs in the layer adsorbed in the air-liquid interface, which causes an increase in the number of monomers adsorbed providing a decrease in surface tension. Results are close to those published by Zhang et al. [44]. It is well-known that the $Br^-$ ion remains more tightly bound to the polar head of the surfactant and is less hydrated than the $Cl^-$ ion, so the former neutralizes the positive charge of the CTAB head groups more than the latter. Our hypothesis is that in formulations with 20 and 50 mol/m$^3$ of salt, part of the $Br^-$ ions remains still associated with the head group attenuating the repulsions between the polar heads of the monomers adsorbed at the interface, so the presence of salt does not have the expected effect on the surface tension decrease. In the formulation with 80 mol/m$^3$ of salt, practically all the $Br^-$ ions have been replaced by the $Cl^-$ ions which are more dissociated, so that the screening effect provided by the presence of $Cl^-$ ions is more effective, facilitating the compaction of the adsorbed layer (increase of $\Gamma_{max}$ and reduction of the $A_{min}$) and the decrease in surface tension. As a result, both effectiveness ($\pi_{CMC}$) and efficiency ($pC_{20}$) increase significantly in the formulation with the highest salt content. Negative values of $\Delta G^0_m$ and $\Delta G^0_{ads}$ indicate that micellization and adsorption are spontaneous processes with higher trend to adsorption than micellization, according with $CMC/C_{20}$ values higher than one.

Data of $D_{ef}$ and $D_s$ for CTAB surface adsorption shown in Table 2 are similar to those published by Zhang et al. [44]. It is observed that $D_{ef}/D_s$ ratio is lower than 1 in formulations with pure water and 20 and 50 mol/m$^3$ NaCl; however, it is close to 1 in the 80 mol/m$^3$ NaCl formulation. This fact suggests that the barrier effects to adsorption are fundamentally of electrostatic character as it decreases in the presence of high salt content.

The NaCl presence affects the CTAB aggregation properties. Fig. 7 shows DLS results of the CTAB dispersions in pure water and with 20 mol/m$^3$ NaCl, after 24 h from their preparation. The absence of micelles can be observed in samples with CTAB concentrations lower than CMC, although large pre-micellar aggregates are observed. Furthermore, in the salt-free formulation (Fig. 7a) a decrease in micelle size is clearly observed when CTAB concentration increases. In the formulations with 20 mol/m$^3$ of NaCl (Fig. 7b) micelles are quite larger than in pure water. It is also observed that the increase in CTAB concentration induces a slight decrease in the size of the micelles and a significant increase in the intensity of the diffracted light. It should be noted that large particles scatter much more light than small ones because the intensity of scattering of a particle is proportional to the sixth power of its diameter. These facts show that in presence of 20 mol/m$^3$ NaCl the increase in CTAB concentration mainly yields the increase in the number of micelles at the expense of the most unstable pre-micellar aggregates, which demonstrates that the presence of salt favors micellization. Fig. 7c shows a larger micelle size with an increasing NaCl concentration due to the increase in its aggregation number. $\zeta$-potential of CTAB dispersions (10 mol/m$^3$ CTAB) in the absence and presence of NaCl, measured after 24 h from their preparation, were 55, 39, 28 and 18 mV, which shows the increasing instability of these

dispersions by increasing the salt content. Backscattered light (BS) of these formulations throughout 32 days are depicted in Fig. S3. They show BS fluctuations in all formulations that indicate lack of homogeneity. The same samples were then analyzed by DLS and ζ-potential. The average sizes were between 225 and 420 nm with very high PDI values (between 0.5 and 0.7), which indicates a high polydispersion in sizes for all formulations after 32 days from their preparation. ζ-potential of these dispersions was between 4 and 5 mV, confirming their loss of stability over time.

### *3.2.2. Effect of NaCl on 20 mol/m³ Span 80 niosomes*

A decrease in CMC and $\gamma_{CMC}$ for the Span 80 surfactant was observed in Table 1 with increasing NaCl concentration. This behavior leads to increasing values of effectiveness ($\pi_{CMC}$) and efficiency ($pC_{20}$), whereas increasing $\Gamma_{max}$ and decreasing $A_{min}$ values are also observed in Table 1 as the salt concentration increases, according to the decrease of $\gamma_{CMC}$. The values of $\Delta G^0_m$ and $\Delta G^0_{ads}$ are very close, indicating that micellization and surface adsorption are spontaneous processes with a similar tendency, regardless of salt concentration, in coherence with the values just higher than the unit of the CMC/$C_{20}$ ratios.

$D_s$ values shown in Table 2 are one order of magnitude less than $D_{ef}$ ones, both in the presence and absence of salt, leading $D_{ef}/D_s$ ratios lower than 10 in all cases. These results reveal the absence of barrier effects to the adsorption at the air-liquid interface, being diffusion the mechanism that controls the interfacial adsorption. However, the fact that $D_{ef} > D_s$ indicates the existence of unstable aggregates in the region near the interface (subsurface) that release monomers, which increasing the driving force for the diffusion of the monomers towards the interface.

Table 3 shows the mean values of the particle diameter, PDI and ζ-potential of the different formulations of Span 80 surfactant after 32 days from their preparation. In the formulations without salt and with 20 mol/m³ of NaCl, low PDI and high ζ-potential absolute values indicate that dispersions, formed by negatively charged niosomes with a size around 200 nm, are stable. Formulations with a high NaCl concentration contain much larger particles (> 0.8 μm) and much more unstable. It must be pointed out that although Span 80 is a non-ionic surfactant, Span 80 niosomes have negative charge (ζ-potential = –42 mV) due to the tendency of hydroxyl groups to adsorb on their surface. $Na^+$ ion has high hydration capacity, so its presence in the formulation medium increases hydrophobic interactions and decreases CMC. The $Na^+$ ions have a stabilizing effect of the niosomal bilayer at low concentration, reducing the volume of the aggregates. However, the presence of a large amount of $Na^+$ ions in the formulations with 50 and 80 mol/m³ of NaCl causes a strong screening effect that weakens the electrostatic repulsions between negatively charged niosomes, thus increasing their instability in suspension and facilitating the formation of large aggregates.

DLS curves of Span 80 suspensions (20 mol/m³) without and with NaCl after 7 days from their preparation are depicted comparatively in Fig. 8. The presence of 200–300 nm diameter niosomes in the formulations without and with 20 mol/m³ of NaCl is observed. The formulation of Span 80 surfactant with 50 mol/m³ NaCl shows particles around 800 nm in size that can be produced by association of niosomes in a medium strongly screened by the presence of salt. In the formulation with 80 mol/m³ of NaCl, the particles show an average size of 300 nm, which indicates much smaller aggregates than those shown in Table 3 for this same formulation. The explanation for this result is probably due to the fact that these aggregates have been formed by the association of Span 80 micelles from the previously breaking of the niosomes in the presence of 80 mol/m³ of NaCl. This hypothesis is based on the S-MLS results shown in Fig. 9, as discussed below.

Fig. 9 depicts BS results of Span 80 formulations recorded for 7 days (Figs. 9a1, 9b1, 9c1 and 9d1) and 32 days (Figs. 9a2, 9b2, 9c2 and 9d2) immediately after their preparation. It is observed that the dispersion without salt is stable for 32 days, with a slight decrease in the height of the foam at the top of the cell. The presence of 20 mol/m$^3$ of NaCl hardly affects BS profiles during the first 7 days (Fig. 9b1); however, for longer times an increase in BS from 20% to 27% is observed (Fig. 9b2) which may be due to the increase in the number of particles in suspension. In formulations with 50 and 80 mol/m$^3$ of NaCl, the BS decreases from 13% to 5% (Fig. 9c2) and from 13% to 11% (Fig. 9d2), respectively, after 32 days from the sample preparation. As stated before, BS is related to the concentration and size of the particles. The BS increases with increasing particle concentration and the size of the aggregates, if they are smaller than the wavelength of the incident light ($\lambda$ = 0.8 μm). However, the BS decreases when the size of the aggregates is greater than the mentioned wavelength. Therefore, the decrease in BS indicates the presence of large particles (> 0.8 μm), together with a smaller amount of particles in suspension. This fact is significant in Fig. 9d2 where accumulation of particles at the bottom of the cell is observed. The small number of particles in the suspension justifies the slight decrease of BS observed in Fig. 9d2 compared to Fig. 9c2. The instability of these formulations is due to the presence of a large quantity of $Na^+$ ions that screen the electrostatic repulsions between negatively charged niosomes, making them unstable in solution. Figs. 9c1 and 9d1 correspond to the BS profiles recorded during the first 7 days. They show the BS decrease (from 12 to 5%) and the increase (from 4 to 15%) in the formulations with 50 and 80 mol/m$^3$ of NaCl, respectively. This behavior indicates, as already mentioned, the presence of particles larger than 0.8 μm in the formulation with 50 mol/m$^3$ of salt. However, the BS increase in Fig. 9d1 indicates the breaking of the niosomes and the proliferation of large number of small Span 80 micelles which, in turn, are unstable and form large aggregates, but smaller than 0.8 microns (as observed in Fig. 8), significantly increasing the BS to values around 15% in Fig. 9d1. This phenomenon, shown in Fig. 9d1, is known as "Ostwald ripening" [48,49]. Results shown in Figs. 9d1 and 9d2 indicate the breakdown of Span 80 niosomes in 80 mol/m$^3$ NaCl solutions and the subsequent formation of large aggregates (> 0.8 μm, see Table 3) that tend to precipitate.

TEM images confirm previous results. They show that in the absence and presence of 20 mol/m$^3$ of NaCl (Figs. 10a and 10b), the niosomes remain independent and stable in solution, with sizes around 200 nm, in agreement with DLS measurements shown in Table 3. The small difference in size between both techniques is due to the fact that in TEM the vesicles adsorbed on the copper grid where the sample is deposited are reduced in size, resulting in slightly smaller aggregate sizes than by DLS [39]. Fig. 10c shows the rupture of the niosomal bilayer in the presence of 50 mol/m$^3$ of NaCl. Fig. 10d shows large aggregates in the formulation with 80 mol/m$^3$ of NaCl that coming from associations of condensed phase after niosomes breakup and are coincident in size with those of Table 3. Moreover, the sample with higher NaCl content is very transparent, indicating the presence of very few particles in suspension due to precipitation of condensates, which justifies the slight decrease of the BS observed in Fig. 9d2, as it was abovementioned.

### *3.2.3. Effect of NaCl on mixed niosomes of Span 80 (20 mol/m$^3$) and CTAB (4 mol/m$^3$)*

Table 1 shows that CMC and $\gamma_{CMC}$ of the Span 80 and CTAB mixed niosomes have intermediate values between those of the pure surfactants. The addition of NaCl hardly changes the CMC value and nevertheless causes a significant decrease of $\gamma_{CMC}$ with respect to the formulation without salt, with similar values in the three salt formulations tested. They show slight increase in the efficiency, $\pi_{CMC}$, and the maximum surface concentration, $\Gamma_{max}$, with respect to the salt-free formulation. Accordingly, a decrease in $A_{min}$ in the presence of electrolyte is observed. Free energy values indicate that both adsorption and micellization are spontaneous processes in all formulations tested, with similar values to those of Span 80 in the absence of CTAB. The CMC/$C_{20}$ ratios close to the unit indicates very similar trends for adsorption and micellization.

The diffusion coefficients, $D_s$ and $D_{ef}$, for these mixed systems are shown in Table 2: they are practically of the same order of magnitude, which disregards the presence of barrier to adsorption at the liquid-air interface.

Table 4 reports the values of size, PDI and ζ-potential of the mixed niosomes after 35 days from their formation. Positive ζ-potentials reveal the adsorption of CTAB in the niosomal bilayer. The low PDI values indicate size homogeneity in all formulations, being lower than those obtained for formulations of single Span 80. Size increases in the presence of 50 and 80 mol/m$^3$ of electrolyte, in accordance with TEM images and BS results, as discussed below.

The variation of BS for mixed niosomes in the absence and presence of NaCl is shown in Fig. 11. Stability in the salt-free formulation (Fig. 11a) and in the presence of 20 mol/m$^3$ of NaCl (Fig. 11b) is observed during the 32 days of testing. The formulation with 50 mol/m$^3$ of NaCl (Fig. 11c) shows slight increase of BS over time (from 16% to 20%) and decrease of particle number in the top of the sample. In the formulation with 80 mol/m$^3$ of NaCl (Fig. 11d), the BS increase is even more marked (from 13% to 20%) and, as in the previous formulation, it is due to the increase in the particle size.

TEM images show spherical mixed niosomes in the salt-free formulation (Fig. 12a), smaller than those of Span 80 alone and stable in dispersion, with no aggregations, corroborating the BS and DLS results. In the presence of 20 mol/m$^3$ of NaCl (Fig. 12b), the TEM image shows small size particles (120 nm) that remain stable in dispersion. In the formulations with 50 and 80 mol/m$^3$ of NaCl (Figs. 12e-12h) niosome associations of irregular form due to physical bonds between neighboring niosomes are observed; however, they are stable in dispersion, without presence of precipitates. Unlike the Span 80 formulation alone, the positive charge of the mixed niosomes, as indicated by the ζ-potential in Table 4, makes them remain stable in the bulk phase.

The aggregation tendency of a mixture of surfactants can be very different from that of pure surfactants. There are different theories and models that describe molecular interaction. According to the theory of regular solutions formulated by Holland and Rubingh [50], the nature and strength of the interaction between two surfactants can be evaluated through the value of the interaction parameter in the formation of mixed aggregates in an aqueous medium ($\beta^M$). The molar fraction of component 1 in the mixed aggregate ($x_1$) and $\beta^M$ can be calculated by solving the following equations:

$$1 = \frac{\left(x_1^M\right)^2 ln\left(\frac{\alpha_1 c_{12}^M}{x_1^M c_1^M}\right)}{\left(1-x_1^M\right)^2 ln\left(\frac{(1-\alpha_1)c_{12}^M}{\left(1-x_1^M\right)c_2^M}\right)} \quad (12)$$

$$\beta^M = \frac{ln\left(\frac{\alpha_1 C_{12}^M}{x_1^M C_1^M}\right)}{\left(1-x_1^M\right)^2} \quad (13)$$

where $C_1^M$, $C_2^M$, and $C_{12}^M$ are the CMC of single and mixed surfactants, respectively. In this work, 1 refers to CTAB, 2 to Span 80, and 12 refers to the 4/20 molar ratio mixture of both surfactants (molar fraction $\alpha_1$ = 0.16). The value of $\beta^M$ can be negative, positive or zero, revealing synergism, antagonism or ideal mixing, respectively, of the surfactants in the formation of aggregates [31] If the behavior is ideal, the CMC of the mixture ($C_{12}^*$) can be described by the following expression [51]:

$$\frac{1}{C_{12}^*} = \frac{\alpha_1}{C_1^M} + \frac{1-\alpha_1}{C_2^M} \quad (14)$$

In a mixture of surfactants, the mixture of hydrophobic chains can be considered as an ideal process in which the free energy of the system decreases when the chain of surfactant moves from a monomeric phase to the aggregates phase. However, interactions between head groups can be considered non-ideal. The difference between $C_{12}^M$ and $C_{12}^*$ is indicative of the non-ideal nature of the interaction [31,46,52]. The molar fraction in the ideal mixture aggregate can be calculated by the following relationship:

$$x_1^* = \frac{\alpha_1 C_2^M}{\alpha_1 C_2^M + (1-\alpha_1) C_1^M} \quad (15)$$

The activity coefficients ($f_1$ and $f_2$) of the surfactants within the aggregates are related to the parameter $\beta^M$ by the following expressions:

$$f_1 = exp[\beta^M (1-x_1)^2] \quad (16)$$

$$f_2 = exp[\beta^M (x_1)^2] \quad (17)$$

Values of $f_1$ and $f_2$ different from the unit indicate no ideality of the mixture in the aggregate. The activity coefficients can be used to calculate the excess free energy of the mixture ($\Delta G_{ex}$) by Eq. 18. Negative values of $\Delta G_{ex}$ reveal that mixed aggregates are more stable than those formed by individual surfactants. Results are reported in Table 5.

$$\Delta G_{ex} = RT[x_1 ln f_1 + (1-x_1) ln f_2] \quad (18)$$

The fulfillment of the following two conditions indicates synergism in the formation of mixed aggregates: $\beta^M < 0$ and $|\beta^M| > |Ln(C_1^M/C_2^M)|$ [53]. This is the case for the salt-free and 20 and 50 mol/m$^3$ NaCl formulations. It means that the attractive interactions between the two component molecules are stronger than the interactions between the same molecules. For these formulations, $C_{12}^M$ is less than $C_{12}^*$ (see Table 1), which means that formation of aggregates occurs at a lower concentration than the ideal mixing. However, in the formulation with 80 mol/m$^3$ of NaCl, $\beta^M > 0$ and $|\beta^M| > |Ln(C_1^M/C_2^M)|$ indicate antagonism, which means that the repulsive forces between the different surfactant molecules are stronger than the repulsive forces between the same surfactant molecules. Furthermore, the $x_1$ values are greater than the $x_1^*$ ones in all formulations, except for the 80 mol/m$^3$ NaCl, indicating that the mixed aggregates are rich in CTAB, compared to the ideal state.

$\Delta G_{ex}$ is negative in all the formulations, except in the 80 mol/m$^3$ NaCl formulation, and its magnitude decreases with the salt content. This suggests that the higher the salt concentration, the less stable

aggregates are formed, which can be explained in terms of electrostatic repulsions between the polar heads of the surfactants in the bilayer, stronger at higher salt concentration

**4. Conclusions**

Surface and aggregation properties of individual and mixed systems of the non-ionic surfactant Span 80 (20 mol/m$^3$) and the cationic surfactant CTAB (4 mol/m$^3$), in salt-free water and in the presence of NaCl (20, 50 and 80 mol/m$^3$) have been studied in this work. The addition of NaCl favors the aggregation process of the CTAB surfactant in large but unstable micelles over time, decreasing the CMC with slight changes in surface tension, except in the presence of 80 mol/m$^3$ of salt where the surface tension is significantly low. Although both the micellization and adsorption processes are spontaneous, the presence of NaCl reduces the barriers to adsorption and is thermodynamically more favored than micellization.

Span 80 niosomes are stable in salt-free formulation and in the presence of 20 mol/m$^3$ of NaCl. Above this salt concentration large aggregates are formed, and in formulations with 80 mol/m$^3$ of NaCl the breaking of niosomes and the formation of Span 80 precipitate occur.

The mixed niosomes of Span 80 (20 mol/m$^3$) and CTAB (4 mol/m$^3$) are positively charged structures. In the absence and presence of low salt concentration (20 mol/m$^3$), the mixed niosomes are spherical, very stable in the bulk, and smaller in size than those of Span 80 alone. However, for high NaCl concentrations (50 and 80 mol/m$^3$), mixed niosomes slightly increase in size due to associations between them, but they remained stable for 32 days in which neither rupture nor formation of precipitates occur. Synergism between surfactants is observed in salt-free water formulations and with 20 and 50 mol/m$^3$ of NaCl, in which the formation of aggregates occurs at a concentration lower than the ideal. For these formulations, the niosomal bilayer is rich in CTAB, compared to the ideal state. Mixed niosomes formulated in presence of 80 mol/m$^3$ of NaCl are unstable over time, and antagonism between surfactants was found in this formulation. These results shed light on the possibility of using CTAB adsorbed on mixed niosomes, taking advantage of its antiseptic and antibacterial properties highly appreciated by the industry, and solving the limitation imposed by its high Krafft temperature.

**Declaration of interests**

The authors declare that they have no known competing financial interests or personal relationships that could have appeared to influence the work reported in this paper.

**Acknowledgments**

This work was supported by Junta de Castilla y León and the European Regional Development Fund (ERDF) through project BU301P18. The authors would like to thank Junta de Castilla y León and the European Social Fund (ESF) for the contract of Davinia Benito-Bedoya through the Youth Employment Initiative (YEI) program, and also to Dr. Carlos Álvarez (Scientific Technical Services, University of Oviedo, Spain) for his valuable help and assistance with TEM measurements.

# CRediT authorship contribution statement

**Lara Roque:** Validation, Investigation, Formal analysis. **María Fernández:** Investigation, Resources. **José M.Benito**: Conceptualization, Formal analysis, Supervision. **Isabel Escudero:** Conceptualization, Project administration, Funding acquisition, Writing - Original Draft, Writing - Review & Editing.

**References**


[1] E. Acosta, Bioavailability of nanoparticles in nutrient and nutraceutical delivery, Curr. Opin. Colloid Interface Sci. 14 (2009) 3–15, https://doi.org/10.1016/j.cocis.2008.01.002

[2] C. Marianecci, L. Di Marzio, F. Rinaldi, C. Celia, D. Paolino, F. Alhaique, S. Esposito, M. Carafa, Niosomes from 80s to present: the state of the art, Adv. Colloid Interface Sci. 205 (2014) 187–206, https://doi.org/10.1016/j.cis.2013.11.018

[3] D.J. McClements, E.A. Decker, Y. Park, J. Weiss, Structural design principles for delivery of bioactive components in nutraceuticals and functional foods, Crit. Rev. Food Sci. Nutr. 49 (2009) 577–606, https://doi.org/10.1080/10408390902841529

[4] M.J. Choi, H.I. Maibach, Liposomes and niosomes as topical drug delivery systems, Skin Pharmacol. Physiol. 18 (2005) 209–219. https://doi.org/10.1159/000086666

[5] L. Roque, I. Escudero, J.M. Benito, Lactic acid recovery by microfiltration using niosomes as extraction agents, Sep. Purif. Technol. 151 (2015) 1–13, https://doi.org/10.1016/j.seppur.2015.07.018

[6] R. Fraile, R.M. Geanta, I. Escudero, J.M. Benito, M.O. Ruiz, Formulation of Span 80 niosomes modified with SDS for lactic acid entrapment, Desalin. Water Treat. 56 (2015) 3463–3475, https://doi.org/10.1080/19443994.2014.993726

[7] L. Roque, I. Escudero, J.M. Benito, Separation of sodium lactate from Span 80 and SDS surfactants by ultrafiltration, Sep. Purif. Technol. 180 (2017) 90–98, https://doi.org/10.1016/j.seppur.2017.02.048

[8] D. Pando, G. Gutiérrez, J. Coca, C. Pazos, Preparation and characterization of niosomes containing resveratrol, J. Food Eng. 117 (2013) 227–234, https://doi.org/10.1016/j.jfoodeng.2013.02.020

[9] S. Chen, S. Hanning, J. Falconer, M. Locke, J. Wen, Recent advances in non-ionic surfactant vesicles (niosomes): fabrication, characterization, pharmaceutical and cosmetic applications, Eur. J. Pharm. Biopharm. 144 (2019) 18–39, https://doi.org/10.1016/j.ejpb.2019.08.015

[10] S. Moghassemi, A. Hadjizadeh, Nano-niosomes as nanoscale drug delivery systems: an illustrated review, J. Control. Release 185 (2014) 22–36, https://doi.org/10.1016/j.jconrel.2014.04.015

[11] Z. Sezgin-Bayindir, N. Yuksel, Investigation of formulation variables and excipient interaction on the production of niosomes, AAPS Pharm. Sci. Technol. 13 (2012) 826–835, https://doi.org/10.1208/s12249-012-9805-4

[12] I.F. Uchegbu, A.T. Florence, Non-ionic Surfactant vesicles (niosomes): physical and pharmaceutical chemistry, Adv. Colloid Interface Sci. 58 (1995) 1–55, https://doi.org/10.1016/0001-8686(95)00242-I

[13] B. Heurtault, P. Saulnier, B. Pech, J.-E. Proust, J.-P. Benoit, Physico-chemical stability of colloidal lipid particles, Biomaterials 24 (2003) 4283–4300, https://doi.org/10.1016/S0142-9612(03)00331-4

[14] S.K. Hait, S.P. Moulik, Determination of critical micelle concentration (CMC) of nonionic surfactants by donor-acceptor interaction with Iodine and correlation of CMC with hydrophile-lipophile balance and other parameters of the surfactants, J. Surfactants Deterg. 4 (2001) 303–309, https://doi.org/10.1007/s11743-001-0184-2

[15] T. Geng, C. Zhang, Y. Jiang, H. Ju, Y. Wang, Synergistic effect of binary mixtures contained newly cationic surfactant: interaction, aggregation behaviors and application properties, J. Mol. Liq. 232 (2017) 36–44, https://doi.org/10.1016/j.molliq.2017.02.055

[16] A. Choucair, A. Eisenberg, Interfacial solubilization of model amphiphilic molecules in block copolymer micelles, J. Am. Chem. Soc. 125 (2003) 11993–12000, https://doi.org/10.1021/ja036667d

[17] M.F. Francis, M. Piredda, F.M. Winnik, Solubilization of poorly water soluble drugs in micelles of hydrophobically modified hydroxypropylcellulose copolymers, J. Control. Release 93 (2003) 59–68, https://doi.org/10.1016/j.jconrel.2003.08.001

[18] S. Paria, P.K. Yuet, Solubilization of naphthalene by pure and mixed surfactants, Ind. Eng. Chem. Res. 45 (2006) 3552–3558, https://doi.org/10.1021/ie051377m

[19] M.R. Behera, S.R. Varade, P. Ghosh, P. Paul, A.S. Negi, Foaming in micellar solutions: effects of surfactant, salt, and oil concentrations, Ind. Eng. Chem. Res. 53 (2014) 18497–18507, https://doi.org/10.1021/ie503591v

[20] B. Naskar, A. Dey, S.P. Moulik, Counter-ion effect on micellization of ionic surfactants: a comprehensive understanding with two representatives, sodium dodecyl sulfate (SDS) and dodecyltrimethylammonium bromide (DTAB), J. Surfactants Deterg. 16 (2013) 785–794, https://doi.org/10.1007/s11743-013-1449-1

[21] D. Kumar, M.A. Rub, Role of cetyltrimethylammonium bromide (CTAB) surfactant micelles on kinetics of $[Zn(II)\text{-}Gly\text{-}Leu]^{+}$ and ninhydrin, J. Mol. Liq. 274 (2019) 639–645, https://doi.org/10.1016/j.molliq.2018.11.035

[22] S. Mahbub, M.A. Rub, Md.A. Hoque, M.A. Khan, Influence of NaCl/urea on the aggregation behavior of dodecyltrimethylammonium chloride and sodium dodecyl sulfate at varying temperatures and compositions: experimental and theoretical approach, J. Phys. Org. Chem. 32 (2018) e3917, https://doi.org/10.1002/poc.3917

[23] M. Rahman, M.A. Khan, M.A. Rub, Md.A. Hoque, A.M. Asiri, Investigation of the effect of various additives on the clouding behavior and thermodynamics of polyoxyethylene (20) sorbitan monooleate in absence and presence of ceftriaxone sodium trihydrate drug, J. Chem. Eng. Data 62 (2017) 1464–1474, https://doi.org/10.1021/acs.jced.6b01027

[24] G. Luo, X. Qi, C. Han, C. Liu, J. Gui, Salt effect on mixed micelle and interfacial properties of conventional cationic surfactants and the ionic liquid surfactant 1-tetradecyl-3-methylimidazolium bromide ([C14mim]Br), J. Surfactants Deterg. 16 (2013) 531–538, https://doi.org/10.1007/s11743-012-1431-3

[25] J.C. Roy, Md.N. Islam, G. Aktaruzzaman, The effect of NaCl on the Krafft temperature and related behavior of cetyltrimethylammonium bromide in aqueous solution, J. Surfactants Deterg. 17 (2014) 231–242, https://doi.org/10.1007/s11743-013-1510-0

[26] M.L. Corrin, W.D. Harkins, The effect of salts on the critical concentration for the formation of micelles in colloidal electrolytes, J. Am. Chem. Soc. 69 (1947) 683–688, https://doi.org/10.1021/ja01195a065

[27] Q. Xu, M. Nakajima, S. Ichikawa, N. Nakamura, P. Roy, H. Okadome, T. Shiina, Effects of surfactant and electrolyte concentrations on bubble formation and stabilization, J. Colloid Interface Sci. 332 (2009) 208–214, https://doi.org/10.1016/j.jcis.2008.12.044

[28] H. Ali, A. Niazi, M.K. Baloch, G.F. Durrani, A. Rauf, A. Khan, Effect of temperature, polymer, and salts on the interfacial and micellization behavior of 3-dodecyl-1-methyl-1*H*-imidazol-3-ium-bromide: a dispersion of a long-chain ionic liquid, J. Dispersion Sci. Technol. 36 (2015) 723–730, https://doi.org/10.1080/01932691.2014.918514

[29] Y. Jiang, T. Geng, Q. Li, G. Li, H. Ju, Influences of temperature, pH and salinity on the surface property and self-assembly of 1:1 salt-free catanionic surfactant, J. Mol. Liq. 199 (2014) 1–6, https://doi.org/10.1016/j.molliq.2014.07.045

[30] K. Nyuta, T. Yoshimura, K. Esumi, Surface tension and micellization properties of heterogemini surfactants containing quaternary ammonium salt and sulfobetaine moiety, J. Colloid Interface Sci. 301 (2006) 267–273, https://doi.org/10.1016/j.jcis.2006.04.075

[31] A. Trawińska, E. Hallmann, K. Mędrzycka, Synergistic effects in micellization and surface tension reduction in nonionic gemini S-10 and cationic RTAB surfactants mixtures, Colloid Surf. A-Physicochem. Eng. Asp. 488 (2016) 162–172, https://doi.org/10.1016/j.colsurfa.2015.10.008

[32] K. Chen, T. Jiao, J. Li, D. Han, R. Wang, G. Tian, Q. Peng, Chiral nanostructured composite films via solvent-tuned self-assembly and their enantioselective performances, Langmuir 35 (2019) 3337–3345, https://doi.org/10.1021/acs.langmuir.9b00014

[33] S. Huo, P. Duan, T. Jiao, Q. Peng, M. Liu, Self-assembled luminescent quantum dots to generate full-color and white circularly polarized light, Angew. Chem. Int. Ed. 56 (2017) 12174–12178, https://doi.org/10.1002/anie.201706308

[34] L. Alonso, L. Roque, I. Escudero, J.M. Benito, M.T. Sanz, S. Beltrán, Solubilization of Span 80 niosomes by sodium dodecyl sulfate, ACS Sustainable Chem. Eng. 4 (2016) 1862–1869, https://doi.org/10.1021/acssuschemeng.6b00148

[35] V.Y. Ixtaina, L.M. Julio, J.R. Wagner, S.M. Nolasco, M.C. Tomás, Physicochemical characterization and stability of chia oil microencapsulated with sodium caseinate and lactose by spray-drying, Powder Technol. 271 (2015) 26–34, https://doi.org/10.1016/j.powtec.2014.11.006

[36] M.I. Capitani, S.M. Nolasco, M.C. Tomás, Stability of oil-in-water (O/W) emulsions with chia (*Salvia hispanica* L.) mucilage, Food Hydrocoll. 61 (2016) 537–546, https://doi.org/10.1016/j.foodhyd.2016.06.008

[37] O. Mengual, G. Meunier, I. Cayré, K. Puech, P. Snabre, TURBISCAN MA 2000: multiple light scattering measurement for concentrated emulsion and suspension instability analysis, Talanta 50 (1999) 445–456, https://doi.org/10.1016/S0039-9140(99)00129-0

[38] D. Velluto, C. Gasbarri, G. Angelini, A. Fontana, Use of simple kinetic and reaction-order measurements for the evaluation of the mechanism of surfactant-liposome interactions, J. Phys. Chem. B 115 (2011) 8130–8137, https://doi.org/10.1021/jp2026187

[39] C. Chen, C. Jiang, C.P. Tripp, Molecular dynamics of the interaction of anionic surfactants with liposomes, Colloid Surf. B-Biointerfaces 105 (2013) 173–179, https://doi.org/10.1016/j.colsurfb.2012.12.045

[40] M. Cócera, O. López, R. Pons, H. Amenitsch, A. de la Maza, Effect of the electrostatic charge on the mechanism inducing liposome solubilization: a kinetic study by synchrotron radiation SAXS, Langmuir 20 (2004) 3074–3079, https://doi.org/10.1021/la035972+

[41] D.K. Chattoraj, K.S. Birdi, Adsorption and the Gibbs Surface Excess, Plenum, New York, 1985.

[42] M.J., Rosen, Surfactants and Interfacial Phenomena, third ed., Wiley-Interscience, New York, 2004.

[43] N. Azum, M.A. Rub, A.M. Asiri, W.A. Bawazeer, Micellar and interfacial properties of amphiphilic drug-non-ionic surfactants mixed systems: surface tension, fluorescence and UV–vis studies, Colloids Surf. A-Physicochem. Eng. Asp. 522 (2017) 183–192, https://doi.org/10.1016/j.colsurfa.2017.02.093

[44] C. Zhang, T. Geng, Y. Jiang, L. Zhao, H. Ju, Y. Wang, Impact of NaCl concentration on equilibrium and dynamic surface adsorption of cationic surfactants in aqueous solution, J. Mol. Liq. 238 (2017) 423–429, https://doi.org/10.1016/j.molliq.2017.05.033

[45] J. Eastoe, J.S. Dalton, Dynamic surface tension and adsorption mechanisms of surfactants at the air-water interface, Adv. Colloid Interface Sci. 85 (2000) 103–144, https://doi.org/10.1016/S0001-8686(99)00017-2

[46] N. Azum, A.Z. Naqvi, M. Akram, Kabir-ud-Din, Studies of mixed micelle formation between cationic gemini and cationic conventional surfactants, J. Colloid Interface Sci. 328 (2008) 429–435, https://doi.org/10.1016/j.jcis.2008.09.034

[47] S. Mahbub, M.R. Molla, M. Saha, I. Shahriar, Md.A. Hoque, M.A. Halim, M.A. Rub, M.A. Khan, N. Azum, Conductometric and molecular dynamics studies of the aggregation behavior of sodium dodecyl sulfate (SDS) and cetyltrimethylammonium bromide (CTAB) in aqueous and electrolytes solution, J. Mol. Liq. 283 (2019) 263–275, https://doi.org/10.1016/j.molliq.2019.03.045

[48] Z. Huang, M. Su, Q. Yang, Z. Li, S. Chen, Y. Li, X. Zhou, F. Li, Y. Song, A general patterning approach by manipulating the evolution of two-dimensional liquid foams, Nat. Commun. 8 (2017) 14110, https://doi.org/10.1038/ncomms14110

[49] Z. Zhang, Z. Wang, S. He, C. Wang, M. Jin, Y. Yin, Redox reaction induced Ostwald ripening for size- and shape-focusing of palladium nanocrystals, Chem. Sci. 6 (2015) 5197–5203, https://doi.org/10.1039/C5SC01787D

[50] P.M. Holland, D.N. Rubingh, Mixed surfactant systems. An overview, in: P.M. Holland, D.N. Rubingh (Eds), Mixed Surfactant Systems, ACS Symposium Series 501, American Chemical Society, Washington DC, 1992, pp. 2–30, https://doi.org/10.1021/bk-1992-0501.ch001

[51] J.H. Clint, Micellization of mixed nonionic surface active agents, J. Chem. Soc., Faraday Trans. 1 71 (1975) 1327–1334, https://doi.org/10.1039/F19757101327

[52] L. Liu, M.J. Rosen, The interaction of some novel diquaternary gemini surfactants with anionic surfactants, J. Colloid Interface Sci. 179 (1996) 454–459, https://doi.org/10.1006/jcis.1996.0237

[53] M.J. Rosen, X.Y. Hua, Dynamic surface tension of aqueous surfactant solutions: 2. Parameters at 1 s and at mesoequilibrium, J. Colloid Interface Sci. 139 (1990) 397–407, https://doi.org/10.1016/0021-9797(90)90114-4

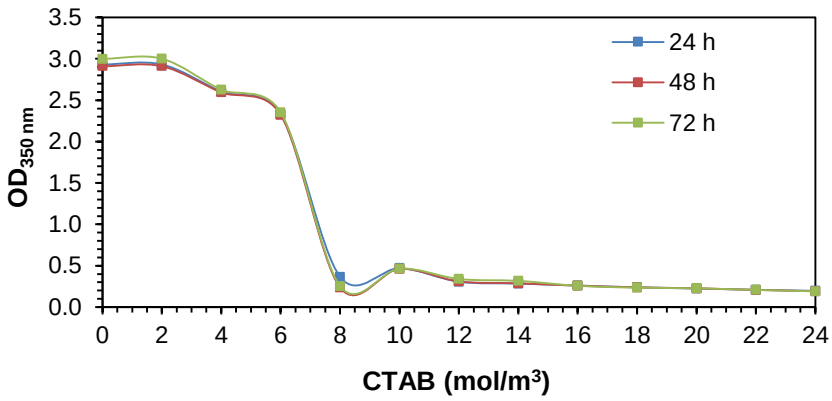


**Figure 1**. Optical density values of 20 mol/m$^3$ Span 80 niosomes in water in presence of CTAB.

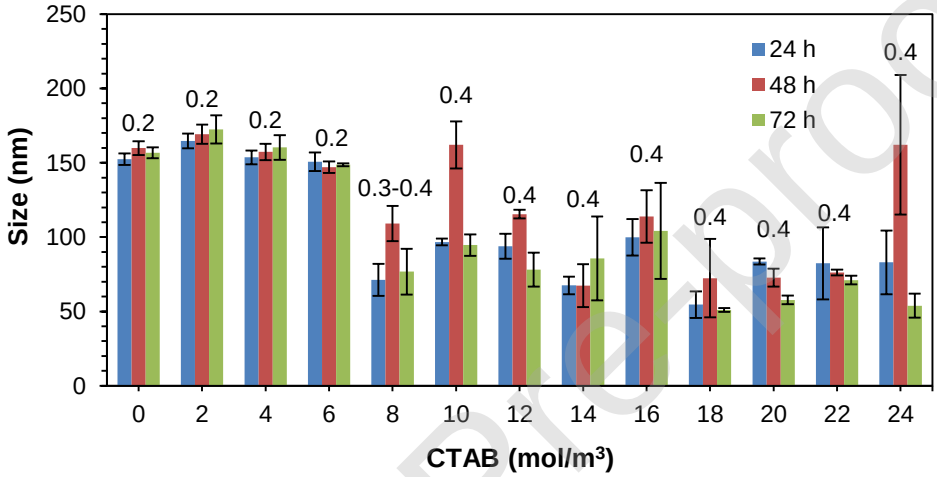


**Figure 2**. Mean hydrodynamic diameter (Z-average) and PDI (data over columns) of 20 mol/m$^3$ Span 80 niosomes in water in presence of CTAB.

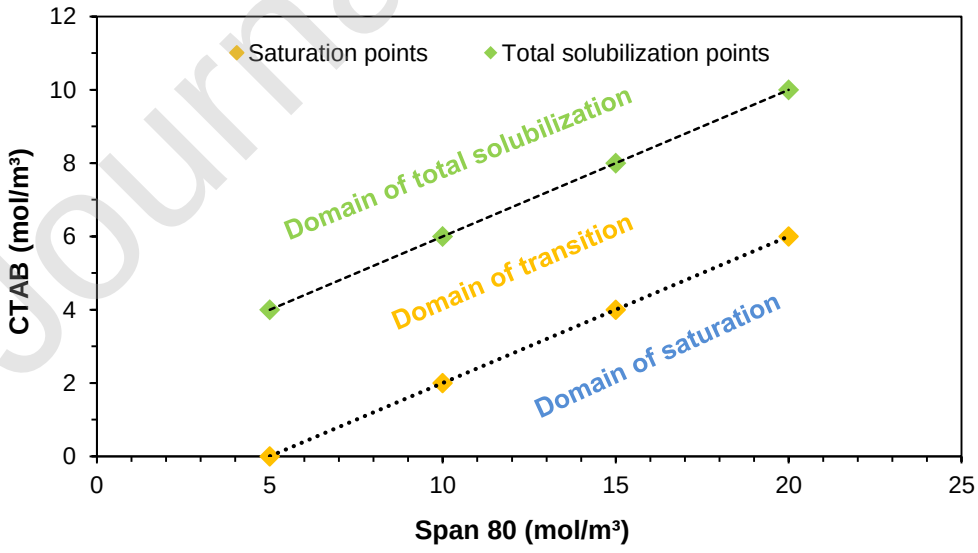


**Figure 3**. Pseudo-phase equilibrium diagram of CTAB – Span 80 niosomes in water.

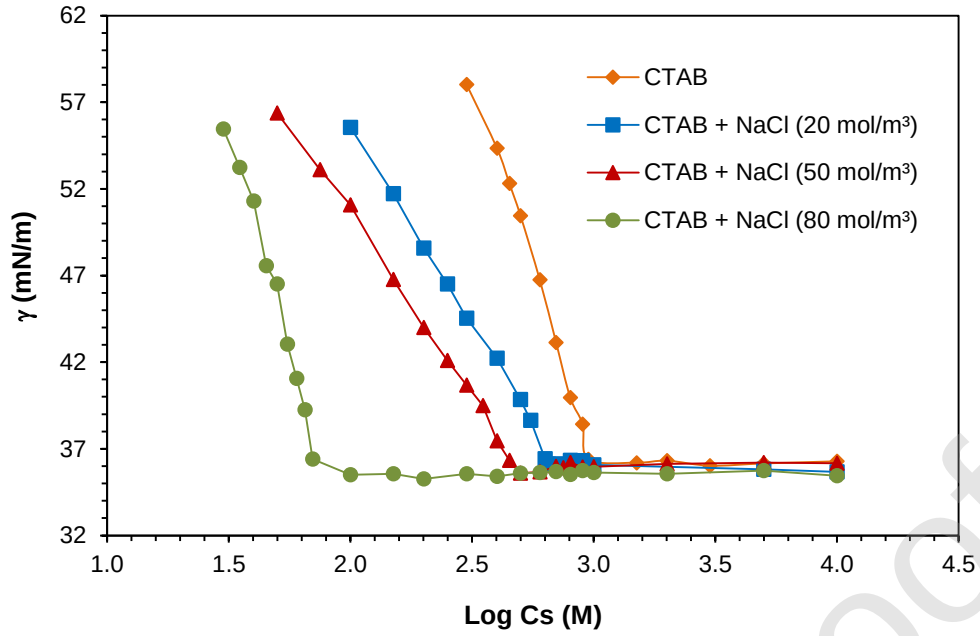


**Figure 4.** Surface tension *vs.* logarithmic concentration of CTAB in pure water and NaCl solutions (20, 50 and 80 mol/m$^3$) at 25 °C.

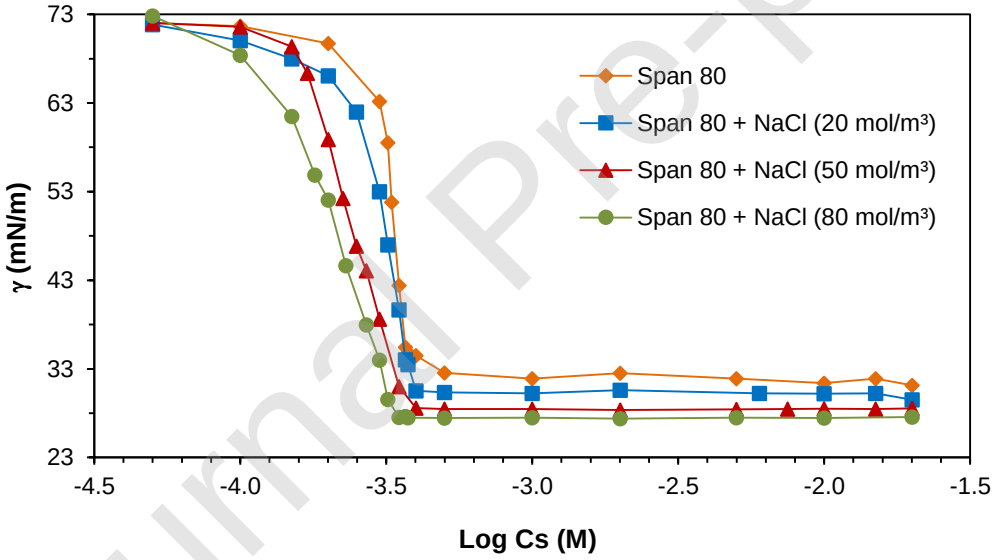


**Figure 5.** Surface tension *vs.* logarithmic concentration of Span 80 in pure water and NaCl solutions (20, 50 and 80 mol/m$^3$) at 25 °C.

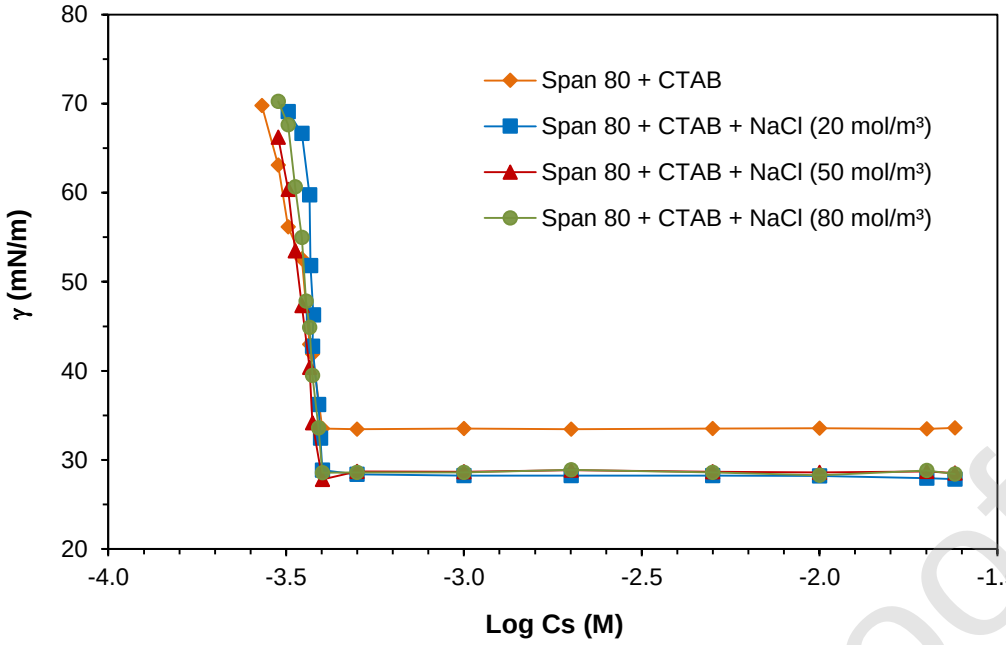


**Figure 6.** Surface tension *vs.* logarithm of the total concentration of surfactants, for mixed formulations of Span 80 and CTAB (4/20 CTAB/Span 80 molar ratio) in pure water and NaCl solutions (20, 50 and 80 mol/m³) at 25 °C.

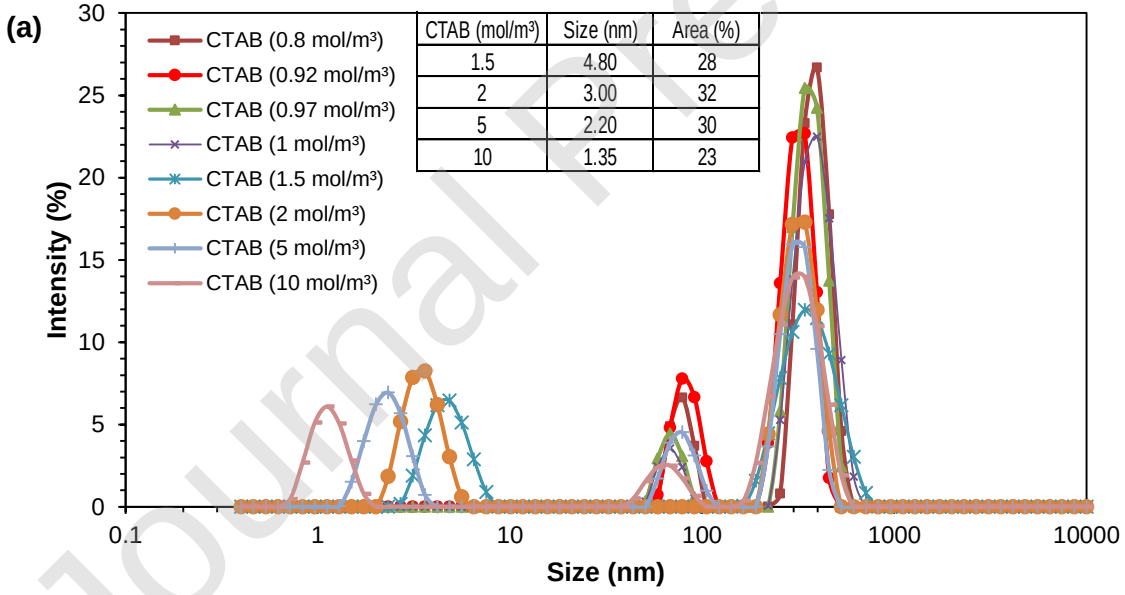

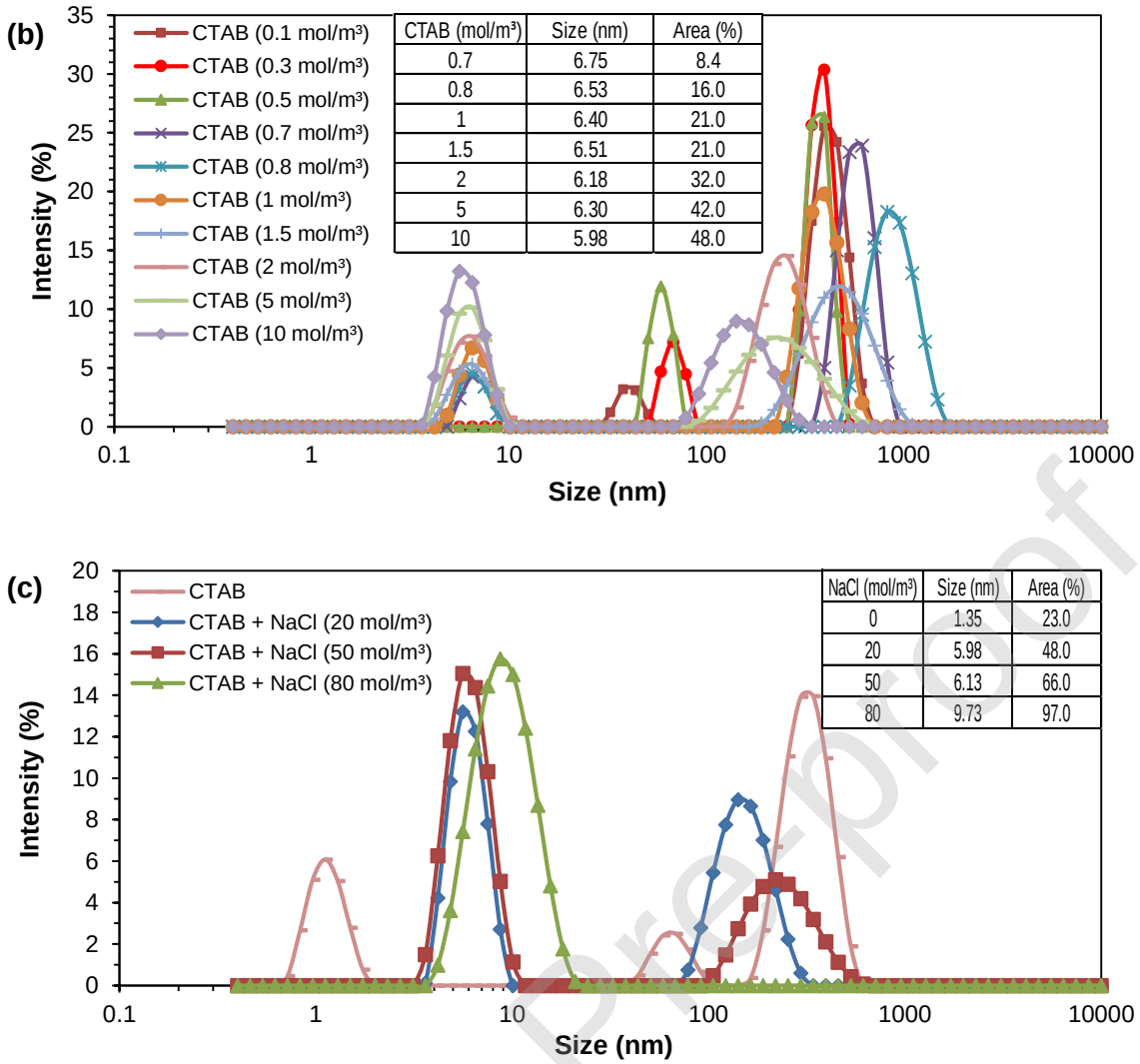


**Figure 7.** DLS results of CTAB dispersions in pure water and in presence of NaCl measured 24 h after formulation. a) CTAB in pure water. b) CTAB in 20 mol/m³ NaCl solutions. c) Formulations of 10 mol/m³ CTAB in pure water and 20, 50 and 80 mol/m³ NaCl solutions. Data in the inserted tables correspond to the small micelles.

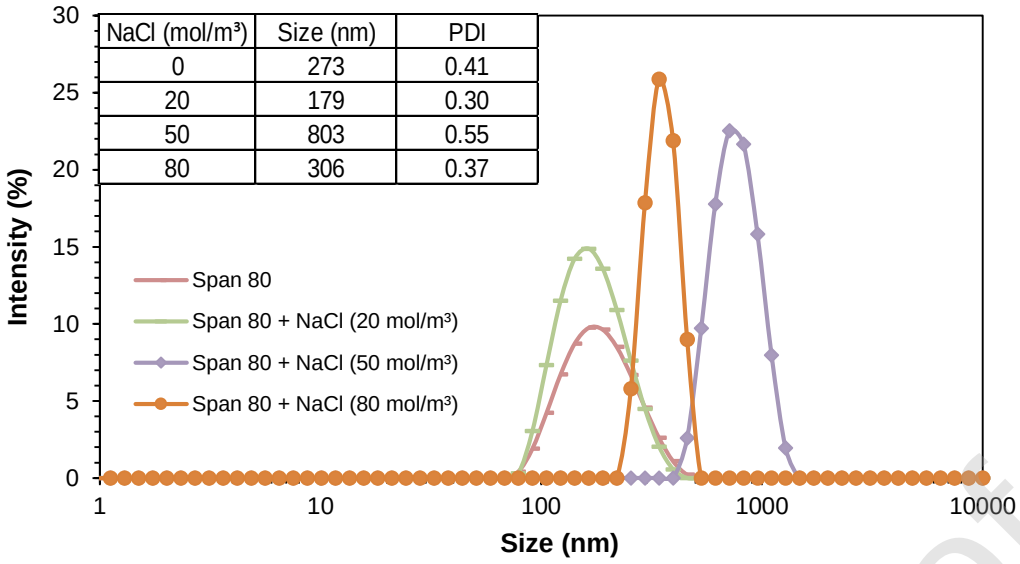


**Figure 8.** DLS results of 20 mol/m³ Span 80 niosomes without and with NaCl (20, 50 and 80 mol/m³) measured 7 days after preparation.

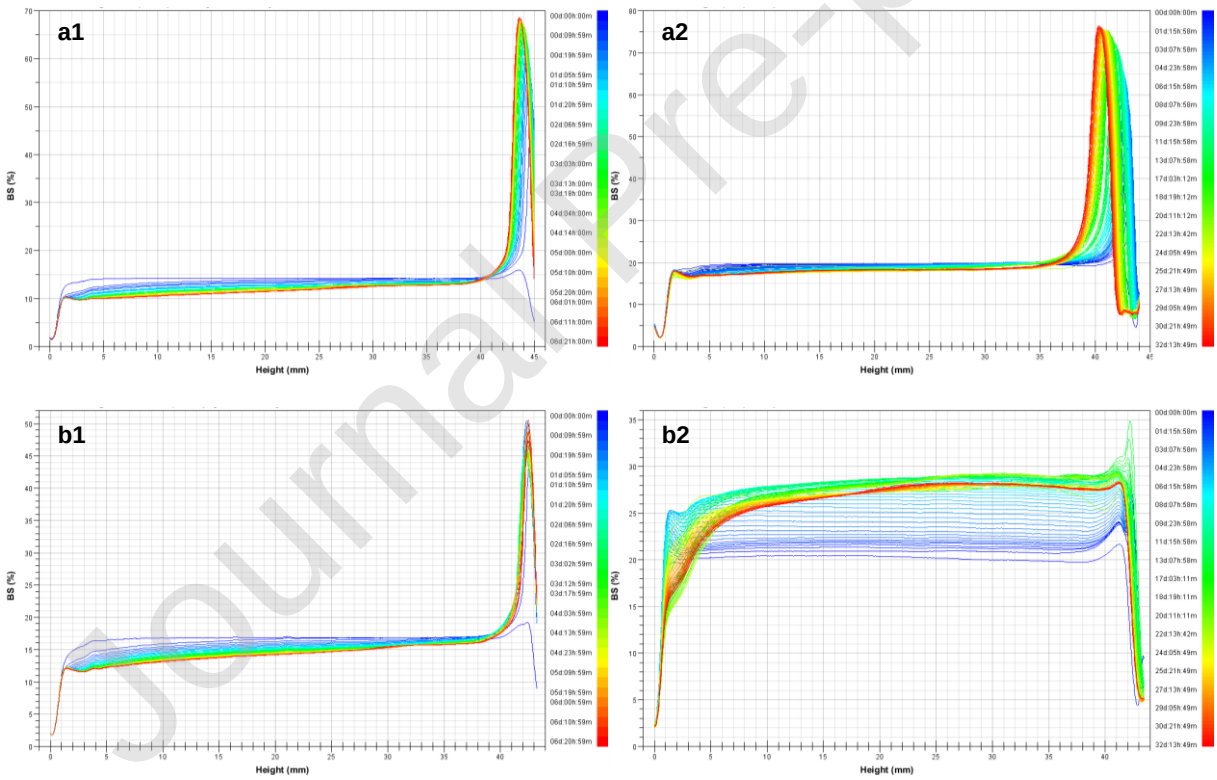

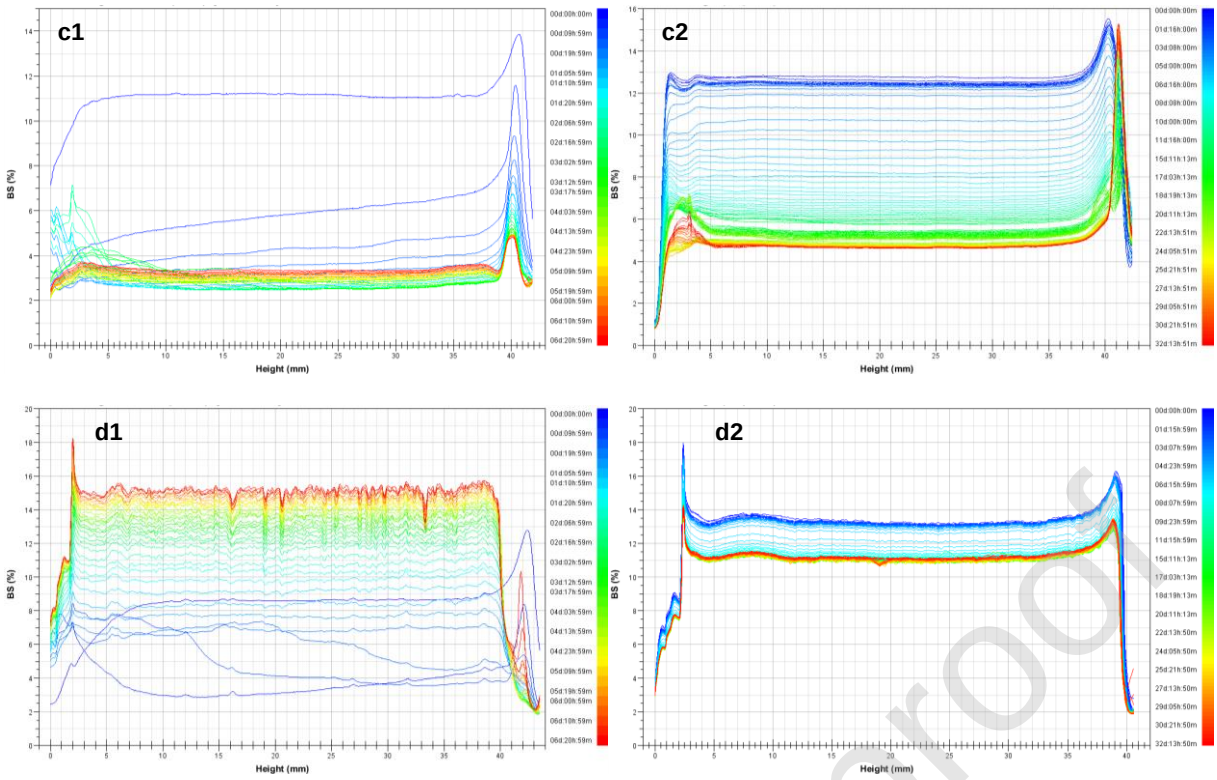


**Figure 9**. Evolution of BS profiles over time for 20 mol/m$^3$ Span 80 niosomes in pure water (a1 and a2) and in 20 (b1 and b2), 50 (c1 and c2) and 80 mol/m³ (d1 and d2) NaCl solutions, measured for 7 days (a1, b1, c1 and d1) and 32 days (a2, b2, c2 and d2) after preparation.

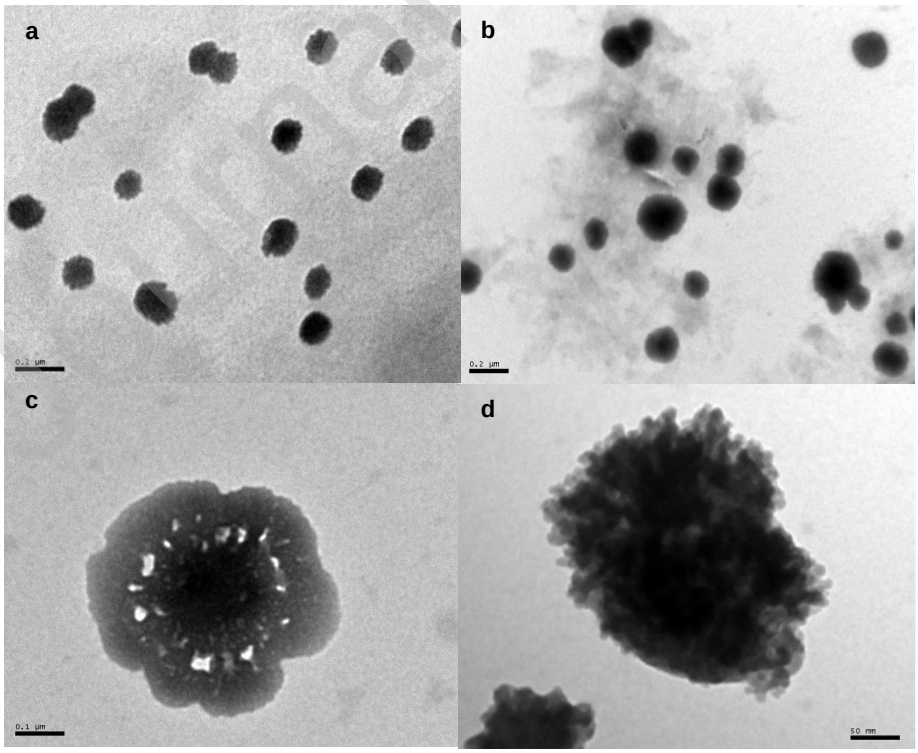

**Figure 10.** TEM images of 20 mol/m$^3$ Span 80 dispersions in pure water (a) and in 20 mol/m$^3$ (b), 50 mol/m$^3$ (c) and 80 mol/m$^3$ (d) NaCl solutions. Scale bars: 0.2 µm (a, b), 0.1 µm (c) and 50 nm (d).

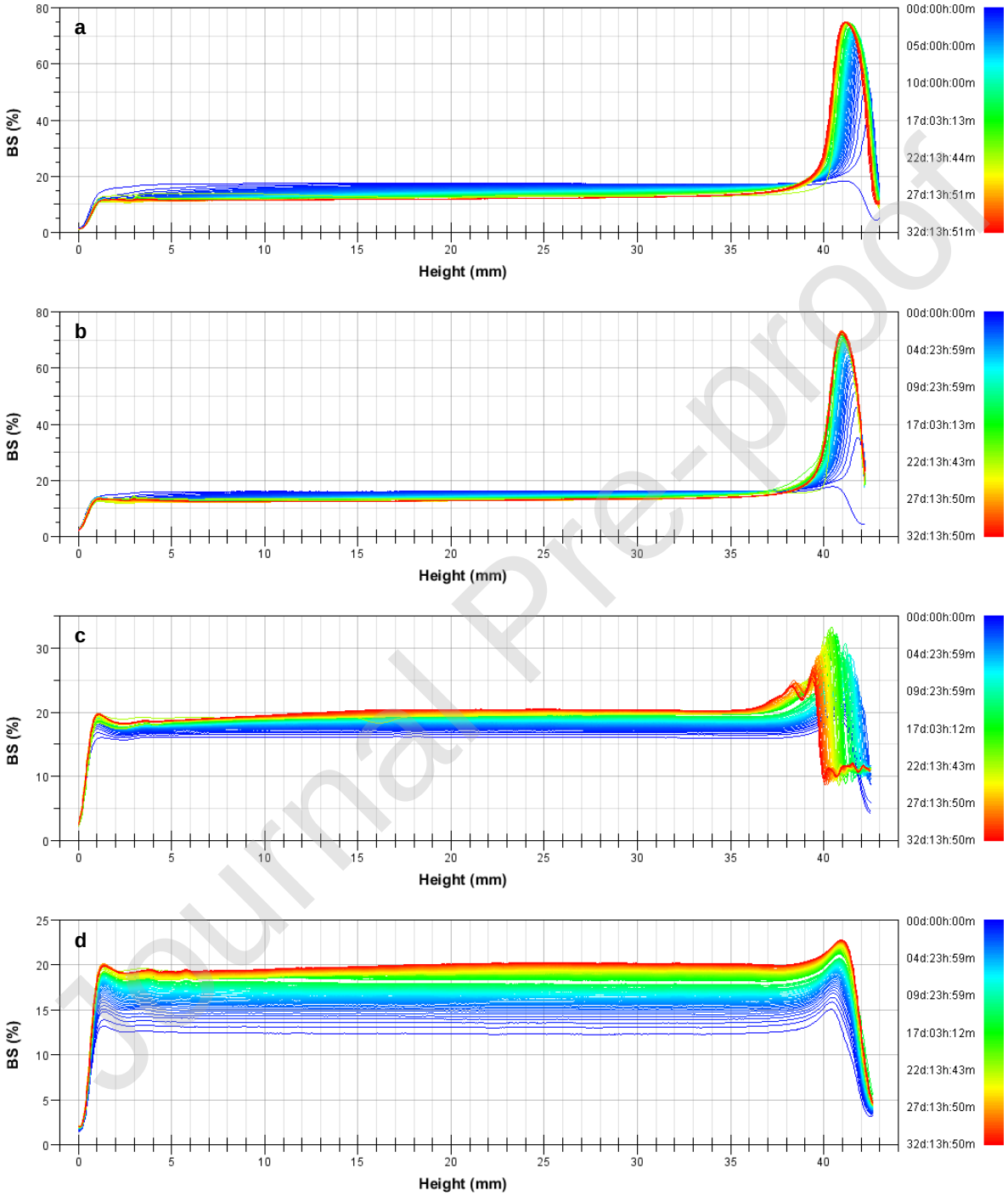

**Figure 11.** Evolution of BS profiles over time for Span 80 (20 mol/m$^3$) and CTAB (4 mol/m$^3$) mixed niosomes in pure water (a) and NaCl solutions: (b) 20 mol/m$^3$, (c) 50 mol/m$^3$, and (d) 80 mol/m$^3$, measured for 32 days after preparation.

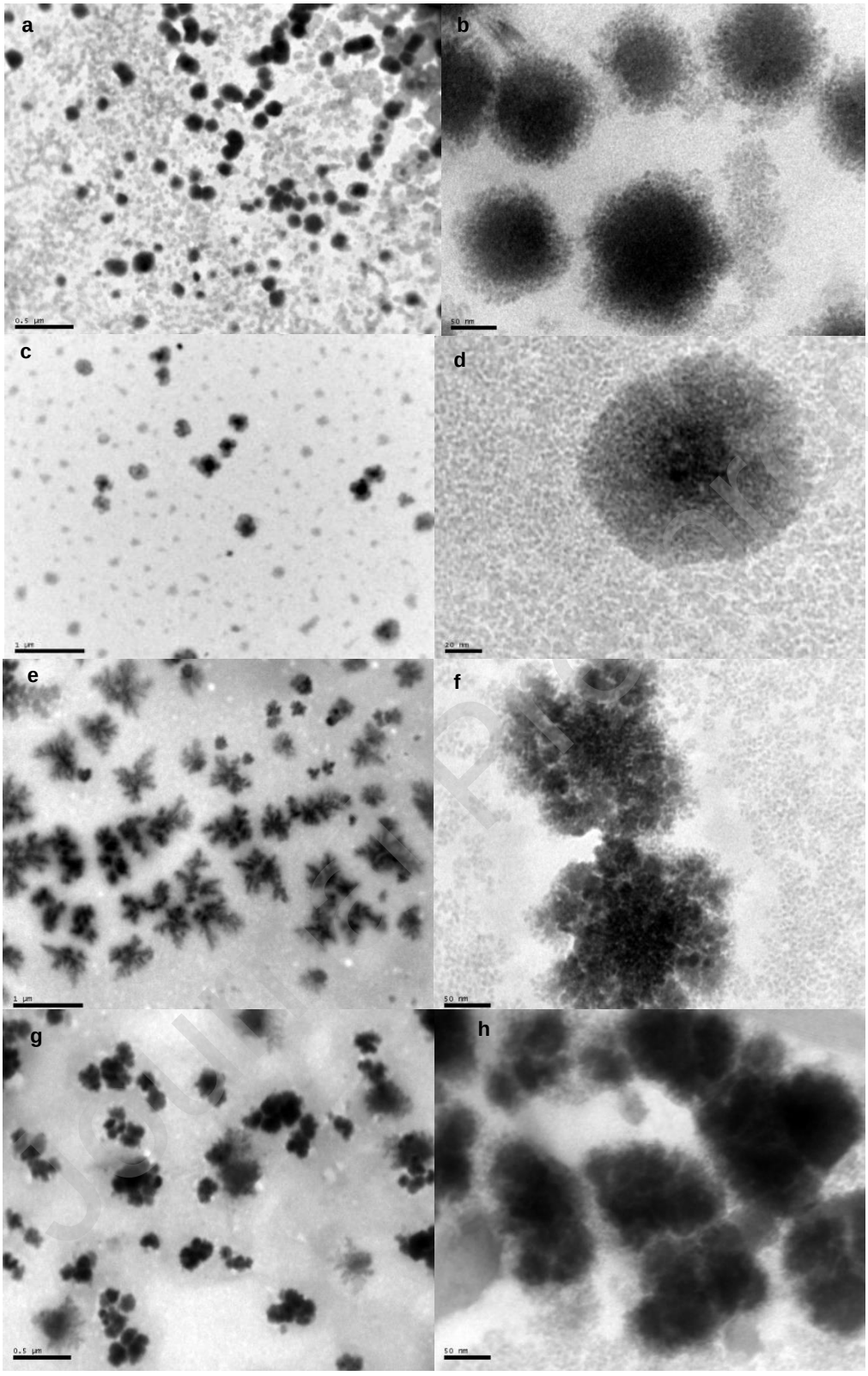

**Figure 12**. TEM images of mixed niosomes of Span 80 (20 mol/$m^3$) and CTAB (4 mol/$m^3$) in pure water (a, b) and in 20 mol/$m^3$ (c, d), 50 mol/$m^3$ (e, f) and 80 mol/$m^3$ (g, h) NaCl solutions. Scale bars: 1 µm (c, e), 0.5 µm (a, g), 50 nm (b, f, h) and 20 nm (d).

**Table 1.** Surface activity parameters of CTAB, Span 80 and CTAB + Span 80 (4/20 molar ratio) in the presence and absence of NaCl at 298 K.

| NaCl (mol/m$^3$) | CMC × $10^3$ (mol/dm$^3$) | $\gamma_{CMC} \times 10^3$ (N/m) | $\pi_{CMC} \times 10^3$ (N/m) | $pC_{20}$ | $CMC/C_{20}$ | $\Gamma_{max}$ (mol/m$^2$) | $A_{min}$ (Å$^2$/molec) | $-\Delta G^0_m$ (kJ/mol) | $-\Delta G^0_{ads}$ (kJ/mol) |
|---|---|---|---|---|---|---|---|---|---|
| **CTAB** | | | | | | | | | |
| 0 | 0.978 | 36.19 | 35.81 | 2.78 | 0.59 | 3.78E-06 | 43.94 | 27.14 | 36.62 |
| 20 | 0.698 | 36.07 | 36.20 | 3.83 | 4.67 | 4.17E-06 | 39.82 | 27.97 | 36.59 |
| 50 | 0.496 | 35.85 | 35.82 | 3.90 | 3.97 | 4.73E-06 | 35.12 | 28.82 | 36.47 |
| 80 | 0.072 | 35.56 | 36.73 | 4.69 | 3.53 | 5.26E-06 | 31.58 | 33.59 | 40.52 |
| **Span 80** | | | | | | | | | |
| 0 | 0.392 | 31.90 | 40.10 | 3.46 | 1.13 | 6.45E-05 | 2.97 | 58.81 | 59.58. |
| 20 | 0.391 | 30.24 | 41.76 | 3.51 | 1.26 | 6.14E-05 | 2.70 | 58.73 | 59.52 |
| 50 | 0.375 | 28.48 | 43.52 | 3.62 | 1.54 | 7.92E-05 | 2.10 | 59.04 | 61.04 |
| 80 | 0.347 | 27.50 | 44.50 | 3.61 | 1.43 | 6.36E-05 | 2.61 | 59.41 | 61.02 |
| **Span 80 + CTAB** | | | | | | | | | |
| 0 | 0.407 | 33.51 | 38.49 | 3.46 | 1.18 | 4.07E-05 | 4.08 | 57.45 | 58.39 |
| 20 | 0.401 | 28.24 | 43.76 | 3.47 | 1.19 | 5.57E-05 | 2.98 | 58.70 | 59.49 |
| 50 | 0.395 | 28.68 | 43.32 | 3.48 | 1.18 | 5.59E-05 | 2.97 | 58.77 | 59.54 |
| 80 | 0.401 | 28.58 | 43.42 | 3.47 | 1.18 | 5.69E-05 | 2.92 | 58.69 | 59.46 |

**Table 2**. Average values of diffusion coefficients $D_s$ and $D_{ef}$ calculated by Eqs. 10 and 11 for the different CTAB, Span 80 and CTAB + Span 80 formulations in the absence and presence of salt.

| Surfactant | NaCl (mol/m³) | $D_s$ (m²/min) | $D_{ef}$ (m²/min) | $D_{ef}/D_s$ | $C_0$ (mol/m³) |
|---|---|---|---|---|---|
| **CTAB** | 0 | 1.10E-11 | 2.18E-12 | 0.20 | 0.5 |
| | 20 | 3.65E-11 | 2.88E-12 | 0.08 | 0.5 |
| | 50 | 5.20E-11 | 2.24E-12 | 0.04 | 0.5 |
| | 80 | 1.28E-11 | 4.53E-11 | 3.55 | 0.5 |
| **Span 80** | 0 | 2.42E-10 | 7.48E-10 | 3.10 | 0.3 |
| | 20 | 2.03E-10 | 1.05E-09 | 5.19 | 0.3 |
| | 50 | 4.00E-10 | 1.47E-09 | 3.68 | 0.3 |
| | 80 | 7.83E-10 | 1.27E-09 | 1.62 | 0.3 |
| **Span 80 + CTAB** | 0 | 7.66E-10 | 1.03E-09 | 1.35 | 0.3 |
| | 20 | 3.02E-10 | 1.48E-09 | 4.89 | 0.3 |
| | 50 | 2.59E-10 | 1.81E-09 | 6.98 | 0.3 |
| | 80 | 7.97E-10 | 2.89E-10 | 2.76 | 0.3 |

**Table 3**. Results of DLS and ζ-potential of 20 mol/m³ Span 80 niosomes measured 32 days after preparation.

| Formulation | Size (nm) | PDI | ζ-potential (mV) |
|---|---|---|---|
| Span 80 without NaCl | 205 | 0.289 | –41.9 |
| Span 80 with 20 mol/m³ NaCl | 179 | 0.151 | –52.4 |
| Span 80 with 50 mol/m³ NaCl | 803 | 0.550 | –17.2 |
| Span 80 with 80 mol/m³ NaCl | 1158 | 0.405 | –12.4 |

**Table 4.** Size, PDI and ζ-potential for the different formulations of the mixed niosomes of Span 80 (20 (mol/m³) and CTAB (4 mol/m³) 32 days after preparation.

| Formulation | Size (nm) | PDI | ζ-potential (mV) |
|---|---|---|---|
| Span 80 + CTAB | 90.16 | 0.276 | 51.0 |
| Span 80 + CTAB + 20 mol/m³ NaCl | 120.6 | 0.252 | 74.8 |
| Span 80 +CTAB + 50 mol/m³ NaCl | 224.6 | 0.293 | 67.7 |
| Span 80 +CTAB + 80 mol/m³ NaCl | 211.1 | 0.262 | 52.3 |

**Table 5.** Physicochemical parameters for Span 80 and CTAB mixed niosomes in pure water and in presence of NaCl, evaluated from surface tension measurements.

| NaCl (mol/m³) | Ln ($C_1^M/C_2^M$) | $X_1^*$ | $C_{12}^*$ (mol/m³) | $X_1$ | $\beta^M$ | $f_1$ | $f_2$ | $\Delta G_{ex}$ (kJ/mol) |
|---|---|---|---|---|---|---|---|---|
| 0 | 0.921 | 0.074 | 0.436 | 0.46 | -6.512 | 0.150 | 0.252 | –4.010 |
| 20 | 0.403 | 0.100 | 0.422 | 0.46 | -4.890 | 0.223 | 0.371 | –2.675 |
| 50 | –1.492 | 0.131 | 0.391 | 0.44 | -3.997 | 0.285 | 0.461 | –2.441 |
| 80 | –1.491 | 0.471 | 0.203 | 0.39 | 2.333 | 2.356 | 1.436 | 1.391 |